Journal of Solid State Chemistry **159,** 413–419 (2001)
doi:10.1006/jssc.2001.9168, available online at http://www.idealibrary.com on IDEAL®

# From Isolated Dimers to an Ordered Antiferromagnetic Ground State in Cation Radical Salts of $Cp_2Mo(dmit)$ with Small Anions ($Br^-$, $BF_4^-$)

Rodolphe Clérac,* Marc Fourmigué,† and Claude Coulon*

*Centre de Recherche Paul Pascal, CNRS UPR 8641, Av. Dr. Schweitzer, 33600 Pessac, France; and †"Sciences Moléculaires aux Interfaces", CNRS FRE 2068, Institut des Matériaux Jean Rouxel, 2, rue de la Houssinière, BP 32229, 44322 Nantes, France
E-mail: clerac@crpp.u-bordeaux.fr, fourmigue@cnrs-imn.fr

Received March 20, 2001; accepted March 21, 2001

IN DEDICATION TO THE LATE PROFESSOR OLIVIER KAHN FOR HIS POINEERING CONTRIBUTIONS TO THE FIELD OF MOLECULAR MAGNETISM

**The structural and magnetic properties of two 1:1 salts of the open-shell $d^1$ organometallic radical cation $Cp_2Mo(dmit)^{+\cdot}$ ($dmit^{2-}$ for 2-thioxo -1,3-dithiole-4,5-dithiolate) with $BF_4^-$ and $Br^-$ are described and analyzed. The two structures differ not only from each other but also from those reported for the three isostructural $PF_6^-$, $AsF_6^-$, $SbF_6^-$ salts with an unfolded $MoS_2C_2$ metallacycle. In $[Cp_2Mo(dmit)][BF_4]$, the $MoS_2C_2$ metallacycle is folded by 23.21(5)° along the S–S hinge and the cations are associated into inversion-centered dimers weakly interacting with each others as reflected by the magnetic susceptibility measurements. In $[Cp_2Mo(dmit)][Br]$, the $MoS_2C_2$ metallacycle is folded by 30.45(4)° and the $Br^-$ anion is involved in C–H ⋯ Br hydrogen bonds. The cations interact antiferromagnetically, giving rise to a three-dimensional set of HOMO–HOMO intermolecular interactions and confirmed by the stabilization of an antiferromagnetic ground state below $T_{Néel} = 4.5$ K.** © 2001 Academic Press

*Key Words:* **crystal engineering; hydrogen bonds; molybdenum; magnetic properties; dithiolene complexes.**

## 1. INTRODUCTION

The noninnocent character of the dithiolene ligand allows its homoleptic bis- or tris(dithiolene) complexes to exhibit sequential reversible one-electron transfer reactions (1), stabilizing open-shell species whose structural and electronic properties strongly depend on the nature of the involved dithiolene ligand (2). In that respect, those containing several sulfur atoms on the dithioethylene core, such as the $dmit^{2-}$ and $dddt^{2-}$ ones ($dddt^{2-}$ for 5,6-dihydro-1,4-dithiine-2,3-dithiolate) (3), have been particularly successful for the elaboration of conducting and superconducting salts (4). These peculiar properties find their origin in extended networks of S ⋯ S interactions between the open-shell species, where a rigid square-planar geometry (for the bis(dithiolene) complexes such as $Ni(dmit)_2^{-\cdot}$) strongly favors $\pi$ stacking (5). On the other hand, the ability of heteroleptic organometallic complexes (6) such as $Cp_2Mo(dmit)$, which combine cyclopentadienyl and $dmit^{2-}$ dithiolene ligands (7), to adapt their geometry to different structural environments has been recently demonstrated in 1:1 salts with various anions of different shape and size. The open-shell $Cp_2Mo(dmit)^{+\cdot}$ cation, in its $TCNQF_4^{-\cdot}$ salt ($TCNQF_4$ for 2,3,5,6-tetrafluoro-7,7,8,8-tetracyano-quinodimethane), exhibits a folding of the $MoS_2C_2$ metallacycle along the S–S hinge (8) and associates into inversion-centered dimers to give rise to novel molecular spin ladders. On the other hand, the salts isolated with the octahedral $MF_6^-$ anions ($PF_6^-$, $AsF_6^-$, or $SbF_6^-$), (9) show an unfolded metallacycle and a three-dimensional set of intermolecular interactions stabilizing an antiferromagnetic ground state below $T_{Néel} = 11.5(2)$ K (in the $PF_6^-$ salt). It was therefore of interest to investigate how the $Cp_2Mo(dmit)^{+\cdot}$ cation will adapt to still smaller anions such as $BF_4^-$ or $Br^-$, and how flexible and tunable are its molecular structure and magnetic properties.

## 2. EXPERIMENTAL

*2.1. Syntheses.* The $Cp_2Mo(dmit)$ donor molecule was prepared as previously described (7). The two salts were grown by the electrocrystallization technique (10) from galvanostatic oxidation of $CH_2Cl_2$ (30 mL) solutions of $Cp_2Mo(dmit)$ (20 mg) in the presence of [*n*-$Bu_4N$][$BF_4$] or [$PPh_4$][Br] as electrolyte (0.05 M) with Pt electrodes (l = 2 cm, Ø = 1 mm). A current intensity of 7 $\mu$A and a temperature of + 5°C was used for $[Cp_2Mo(dmit)][BF_4]$, 5 $\mu$A and − 10°C for $[Cp_2Mo(dmit)][Br]$. Crystals were harvested on the anode after one week and washed with a small amount of pure $CH_2Cl_2$.

*2.2. Structural studies.* Details about data collection and solution refinement are given in Table 1. Data were



0022-4596/01 $35.00

**TABLE 1**
**Crystallographic Data**

| | $[Cp_2Mo(dmit)][BF_4]$ | $[Cp_2Mo(dmit)][Br]$ |
|---|---|---|
| Formula | $C_{13}H_{10}BF_4MoS_5$ | $C_{13}H_{10}BrMoS_5$ |
| Formula mass | 509.26 | 502.36 |
| Crystal dimensions ($mm^3$) | $0.4 \times 0.04 \times 0.008$ | $0.32 \times 0.32 \times 0.02$ |
| Crystal system | Monoclinic | Monoclinic |
| Space group | $P2_1/c$ | $P2_1/c$ |
| $a$ (Å) | 6.5208(6) | 16.6921(13) |
| $b$ (Å) | 15.1924(14) | 7.2960(4) |
| $c$ (Å) | 16.9502(14) | 12.8445(10) |
| $\beta$ (°) | 93.534(10) | 96.222(8) |
| $V$ (Å$^3$) | 1676.0(2) | 1555.1(2) |
| $Z$ | 4 | 4 |
| Temperature (K) | 293 | 293 |
| $d_{calc}$ ($g\,cm^{-3}$) | 2.018 | 2.146 |
| $\mu$ ($mm^{-1}$) | 1.439 | 4.068 |
| Diffractometer | Stoe-IPDS | Stoe-IPDS |
| Absorpt. corr. | Empirical (multiscan) | Empirical (multiscan) |
| Data collected | 9652 | 10,677 |
| Independent data | 2595 | 2941 |
| $R_{int}$ | 0.1407 | 0.0593 |
| Observed data ($I > 2\sigma(I)$) | 1442 | 2021 |
| Param. refined | 202 | 181 |
| $R(F)$ | 0.0462 | 0.0331 |
| $wR(F^2)$ | 0.0863 | 0.0746 |
| GoF(obs) | 0.976 | 0.976 |
| Residual $d$ (e Å$^{-3}$) | 0.80, −0.67 | 0.628, −0.761 |

collected on a Stoe-IPDS Imaging Plate system at room temperature operating with a Mo$K\alpha$ X-ray tube with a graphite monochromator. The structures were solved (SHELXS) by direct methods and refined (SHELXL-93) by full-matrix least-squares methods. Empirical absorption corrections were applied. Hydrogen atoms were introduced at calculated positions (riding model), included in structure factor calculations, and not refined. Crystallographic data have been deposited, in CIF format, with the Cambridge Crystallographic Data Centre as CCDC 156241 and 156242 for $[Cp_2Mo(dmit)][BF_4]$ and $[Cp_2Mo(dmit)][Br]$, respectively.

*2.3. Magnetic studies.* Magnetic susceptibility measurements were obtained with the use of a Quantum Design SQUID magnetometer MPMS-5. Data were collected from 1.8 to 300 K on finely divided polycrystalline samples (10.83 mg for $[Cp_2Mo(dmit)][BF_4]$ and 17.00 mg for $[Cp_2Mo(dmit)][Br]$). The data were corrected for the sample holder and for the diamagnetic contribution calculated from Pascal constants (11).

EPR experiments were performed on oriented single crystals on a Bruker ESP300E spectrometer equipped with an ESR900 cryostat (4.2–300 K) from Oxford Instruments.

*2.4. Extended Hückel calculations.* Tight binding calculations are based on the effective one-electron Hamiltonian of the extended Hückel method (12). The off-diagonal matrix elements of the Hamiltonian were calculated according to the modified Wolfsberg–Helmholz formula (13). The basis set consists of double-$\zeta$ Slater-type orbitals for Mo, S, and C and single-$\zeta$ Slater-type orbitals for H. The exponents, contraction coefficients, and atomic parameters have been taken from previous work (7).

## 3. RESULTS AND DISCUSSION

The two 1:1 salts were obtained upon electrocrystallization of $Cp_2Mo(dmit)$, as described with other counter anions ($PF_6^-$, $AsF_6^-$, $SbF_6^-$) (10). While the $BF_4^-$ salt crystallizes into very thin needles, the bromide anion afforded thick plates, a preliminary indication of different structures despite the comparable anion sizes, as confirmed by their X-ray structure resolution (Table 1). Indeed, the two structures are not only different from each other but also from the orthorhombic structures described with the octahedral $PF_6^-$, $AsF_6^-$, or $SbF_6^-$ anions, which give rise to elongated plates. $[Cp_2Mo(dmit)][BF_4]$ crystallizes in the monoclinic system, space group $P2_1/c$, with both the $Cp_2Mo(dmit)^{+\cdot}$ radical cation and the $BF_4^-$ anion in general position in the unit cell (Fig. 1). Bond lengths within $Cp_2Mo(dmit)^{+\cdot}$ (Table 2) confirm the oxidized character with the typical shortening of the C–S and concurrent lengthening of the central C=C bond when compared with the neutral, un-

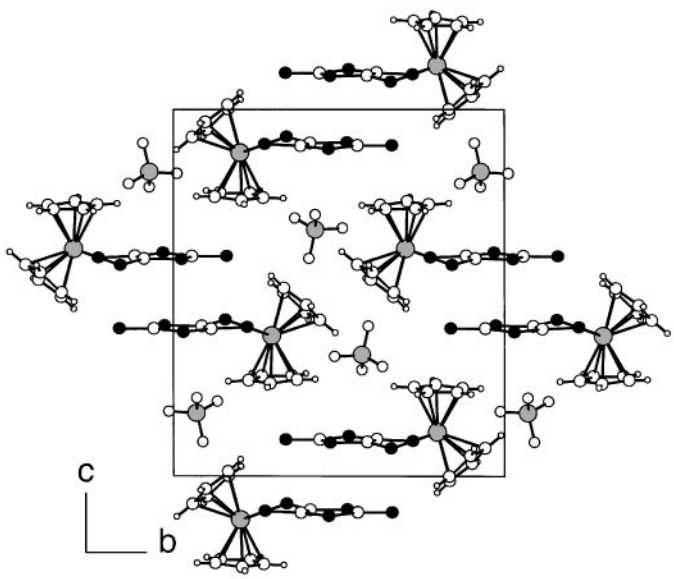


**FIG. 1.** A projection view of $[Cp_2Mo(dmit)][BF_4]$ along $a$ showing the inversion-centered dimers.

**TABLE 2**
**Important Bond Distances and Angles in the Two Salts and the Neutral $Cp_2Mo(dmit)$ as Reference Compound (23)**

| | $Cp_2Mo(dmit)$ neutral | $[Cp_2Mo(dmit)][BF_4]$ | $[Cp_2Mo(dmit)][Br]$ |
|---|---|---|---|
| Mo–S | 2.457(3) | 2.432(2) | 2.4434(12) |
| C–S(–Mo) | 1.745(9) | 1.718(8) | 1.712(5) |
| C=C | 1.357(12) | 1.360(10) | 1.385(6) |
| S–Mo–S | 83.95(8) | 83.03(7) | 82.73(4) |
| Folding angle ($\theta$) | 4.2(1) | 23.21(5) | 30.45(4) |

oxidized donor molecule. The $MoS_2C_2$ metallacycle is folded by 23.21(5)°. In the solid state, the radical cations are associated into inversion-centered dimers (Fig. 1) with a plane-to-plane distance (between dmit moieties) of 3.718(4) Å. These dimers are essentially isolated from each other, as confirmed by the calculations of $\beta_{\text{HOMO-HOMO}}$ interaction energies (14). While the intradimer $\beta$ value amounts to 0.13 eV ($2t = 0.17$ eV, $2t$ is the energy difference between the two highest occupied orbitals of the dimeric unit), the other interactions along the $a$ axis and between the chains running along $a$ do not exceed 0.04 eV ($2t < 0.07$ eV). The temperature dependence of the magnetic susceptibility obtained on a polycrystalline sample of the $BF_4^-$ salt is presented in Fig. 2. The magnetic susceptibility increases from room temperature to reach a rounded maximum at about 170 K, and then decreases dramatically down to 50 K. This behavior, confirmed by preliminary EPR measurements, is typically seen for isolated dimers of $S = \frac{1}{2}$ magnetic spin (with an antiferromagnetic interaction within the dimer), as one would have expected regarding the crystallographic data previously presented. At lower temperature, the compound is diamagnetic; i.e., only the singlet ground state ($S = 0$) is populated. By increasing the temperature, a part of the magnetic spin population reaches the triplet excited state ($S = 1$), which increases the magnetic susceptibility. The theoretical expression for the magnetic susceptibility of an antiferromagnetic coupled $S = \frac{1}{2}$ dimer is well represented by the Bleaney–Bowers equation (15)

$$\chi_{\text{dimer}} = \frac{2Ng^2\mu_B^2}{k_B T(3 + \exp(-2J/k_B T))}, \qquad [1]$$

where $N$, $\mu_B$ and $k_B$, have their usual meanings, $g$ is the Landé factor of the Mo complex, and $J$ is the magnetic exchange constant between paramagnetic ions ($S = \frac{1}{2}$) in the dimer ($H = -2JS_1 \cdot S_2$). A second superposed magnetic contribution is observed (see Fig. 2); the increase in the susceptibility value in the lowest temperature region is usually seen in these dimer systems (which present a singlet ground state). This Curie–Weiss-type behavior (second part of the following equation) is associated with the presence of small amounts of paramagnetic impurities,

$$\chi = (1 - \rho)\chi_{\text{dimer}} + \frac{\rho N\mu_B^2}{k_B(T - \theta)} + \chi_{\text{dia}}, \qquad [2]$$

where $\chi_{\text{dia}}$ is the diamagnetic contribution and $\rho$ represents the fraction of paramagnetic impurity ($g_{\text{imp}} = 2$). The experimental data does not fit very well to Eq. [2] (see Fig. 2, dotted line); the best set of parameters found is $J/k_B = -140$ K, $\rho = 1.3\%$, $\theta = -16$ K (the $g$ value was fixed at 2, which is a good average value for $Cp_2Mo(dmit)^{+\cdot}$ (9) and confirmed at room temperature by EPR measurements). To reproduce the magnetic susceptibility measurements observed, we took into account the complex network of much weaker magnetic interactions between the dimers. These interactions were introduced in the model by the mean-field approximation (16)

$$\chi = (1 - \rho)\frac{\chi_{\text{dimer}}}{1 - (4zJ'\chi_{\text{dimer}}/Ng^2\mu_B^2)} + \frac{\rho N\mu_B^2}{k_B(T - \theta)} + \chi_{\text{dia}}, \qquad [3]$$

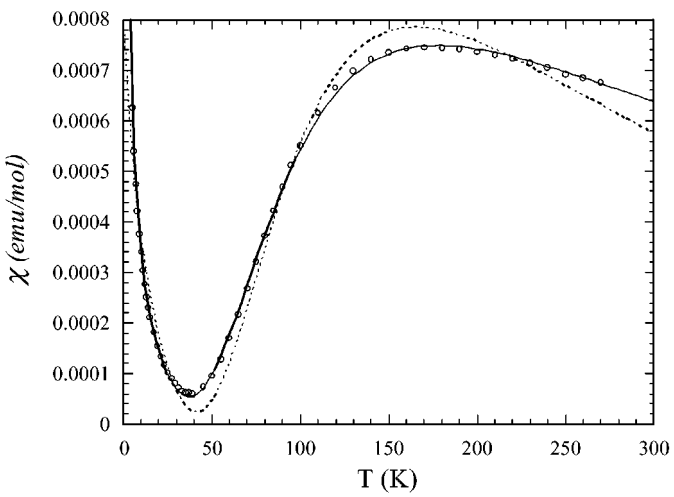


**FIG. 2.** Temperature dependence of the magnetic susceptibility for $[Cp_2Mo(dmit)][BF_4]$ at 5000 G. The dotted and solid lines are the best fits obtained using Eqs. [2] and [3], respectively.

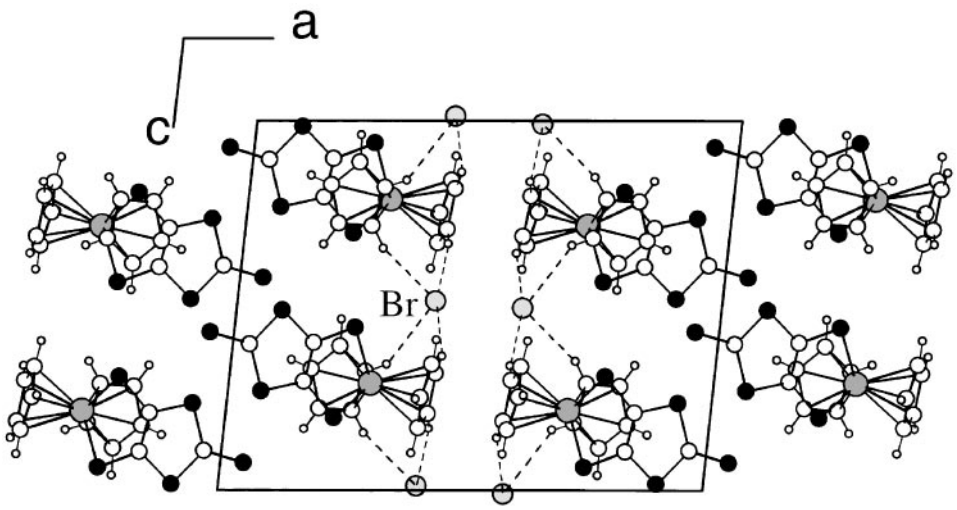


**FIG. 3.** A projection of $[Cp_2Mo(dmit)][Br]$ along the $b$ axis. The C–H $\cdots$ Br hydrogen bonds are represented with dashed lines.

where $z$ is the number of dimer's next neighbors ($z = 6$) and $J'$ is the average of interdimer magnetic exchange constants. An excellent agreement with the experimental data was found with this model that yields $J/k_B = -145$ K, $J'/k_B = -15$ K, $\rho = 1.4\%$, $\theta = -2.5$ K (solid line in Fig. 2). In a Hubbard model, the exchange interaction is directly related to $2t$ ($J \approx 2t^2/U$, where $U$ is the intrasite electronic repulsion term). The $J$ ($-145$ K) and $J'$ ($-15$ K) values obtained from the fitting of the magnetic data compare qualitatively well to the theoretical values (167 K and $< 28$ K respectively) from the calculated $2t$ and a standard $U = 1$ eV (17). These results are consistent with the above crystallographic description, i.e., the consideration of Mo complexes dimers weakly interacting with their nearest neighbors in a three-dimensional fashion.

$[Cp_2Mo(dmit)][Br]$ crystallizes in the monoclinic system, space group $P2_1/c$ with both $Cp_2Mo(dmit)^{+\cdot}$ radical cation and bromide anion in general position in the unit cell (Fig. 3) with a noticeable segregation between the bromide anions, enclathrated between the Cp anions through four short and directional C–H $\cdots$ $Br^-$ hydrogen bonds (Table 3). Such weak hydrogen bonds (18) have been shown to be particularly effective at controlling the solid state structures of organic or organometallic (19) moieties with halide anions (20). We indeed observed here that the aromatic $sp^2$ C–H moieties of the cyclopentadienyl ligands are most probably activated by the oxidized character of the complexes, as already observed in several tetrathiafulvalenium salts (21, 22). It is also important to note that within the organometallic slabs, the $MoS_2C_2$ metallacycle is even more folded than that in $[Cp_2Mo(dmit)][BF_4]$ with $\theta = 30.45(4)^\circ$, in sharp contrast with the structures of the $PF_6^-$, $AsF_6^-$, or $SbF_6^-$ anions where the metallacycle is fully planar. This striking structural variability finds its origin in an electronic stabilization through a symmetry-allowed $Cp_2Mo$/dithiolene fragment orbital mixing in the folded conformation. We have also shown that in $Cp_2Mo(dmit)$, the energy cost for folding (23) in the $d^1$ oxidized state was very small; hence the various geometries are dependent upon the nature of the counteranion with a folding angle varying between $0^\circ$ and $35^\circ$. As shown in Fig. 4, each open-shell organometallic complex interacts in the solid state through short S $\cdots$ S contacts with the neighboring molecules in the $(b, c)$ layers (interactions I–III) while interaction IV through the Cp $\cdots$ Cp overlap connects these layers in the $a$ direction, giving rise to a isotropic set of intermolecular overlap interactions comprised between 0.0165 and 0.0572 eV ($2t(I) = 0.0572$ eV, $2t(II) = 0.0334$ eV, $2t(III) = 0.0200$ eV, $2t(IV) = 0.0165$ eV and $\Sigma J/k_B \approx 30$ K where $\Sigma J$ is the sum of the calculated $J$ from the $2t$ values).

EPR experiments on an oriented single crystal confirm the paramagnetic nature of the $[Cp_2Mo(dmit)][Br]$ salt. A single Lorentzian line is systematically observed in the whole temperature range down to 4.2 K. Its integration gives a good estimation of the temperature dependence of

**TABLE 3**
**C–H $\cdots$ Br Hydrogen Bond Characteristics in $[Cp_2Mo(dmit)][Br]$**

| | (C–)H $\cdots$ Br (Å) | C(–H) $\cdots$ Br (Å) | C–H $\cdots$ Br (°) |
|---|---|---|---|
| Br1 $\cdots$ H8[a] | 2.802 | 3.702(6) | 163.18 |
| Br1 $\cdots$ H7 | 2.841 | 3.629(6) | 143.22 |
| Br1 $\cdots$ H11[a] | 2.902 | 3.806(6) | 164.49 |
| Br1 $\cdots$ H10 | 2.931 | 3.825(6) | 161.92 |

*Note.* Only H $\cdots$ Br distances shorter than 4 Å have been reported.
[a] i $x, -\frac{1}{2} - y, -\frac{1}{2} - z$.

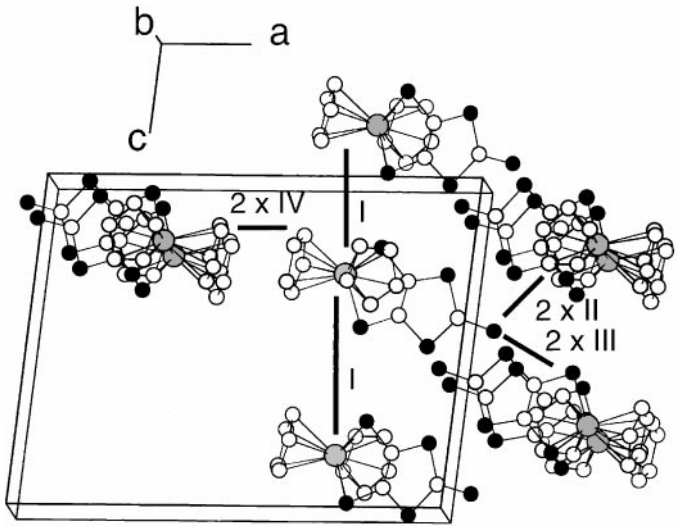


**FIG. 4.** View of the magnetic interaction network for $[Cp_2Mo(dmit)][Br]$.

the magnetic susceptibility, which follows a Curie–Weiss law down to 30 K with a Weiss constant around $-20$ K. This clearly indicates the antiferromagnetic nature of the magnetic interaction between the spin carriers (radical cations). At low temperature, the susceptibility reaches a maximum around 11 K, then decreases dramatically as often observed close to an antiferromagnetic transition. A more accurate description of the magnetic susceptibility by static method (SQUID magnetometer) will be presented in detail below. At room temperature the eigenvalues of the $g$ tensor were determined by rotation figures in the principal planes, taking into account that one of them is found along the monoclinic axis $b$ ($g_b = 2.0091$) for symmetry reasons (24). The others are localized in the perpendicular plane ($a, c^*$). Due to positions of the radical cations in the structure, and not by a symmetry argument as for the $b$ axis, the $a$ and $c^*$ directions are principal magnetic directions for the $g$ tensor: $g_a = 2.0165$ and $g_{c^*} = 1.9927$. Those values are close to those observed for the related family of materials $[Cp_2Mo(dmit)][MF_6]$ (9). The temperature dependence of the $g$ factor, along $b$, is shown in Fig. 5, with a slight decrease from 2.0091 to 2.0086 between 300 and 50 K respectively. Below this quasi-constant regime, $g$ increases to reach a maximum around 7 K at 2.0105, then decreases again between 7 and 4.9 K down to 2.0062. Close to the lowest available temperature 4.2 K, the $g$ factor increases rapidly. In the same direction, the thermal behavior of the linewidth ($\Delta H$) is similar to the $g$ factor one, especially in the low-temperature part. After a continuous increase, from 84 G at room temperature to a maximum at 178 G around 9 K, a decrease of $\Delta H$ to 110 G is observed down to 4.8 K. Then as for the $g$ factor, a rapid increase down to the lowest temperature available (4.2 K) is noted. These low-temperature features on the $g$ factor and the $\Delta H$, correlated to the decrease of the resonance line intensity (susceptibility), have been already observed in the $MF_6$ salts before the antiferromagnetic transition (9). This situation seems to indicate that an antiferromagnetic order is stabilized close to 4.2 K in $[Cp_2Mo(dmit)][Br]$. Static magnetic susceptibility measurements were performed down to 2 K to confirm this assumption. As shown in Fig. 6, $[Cp_2Mo(dmit)][Br]$

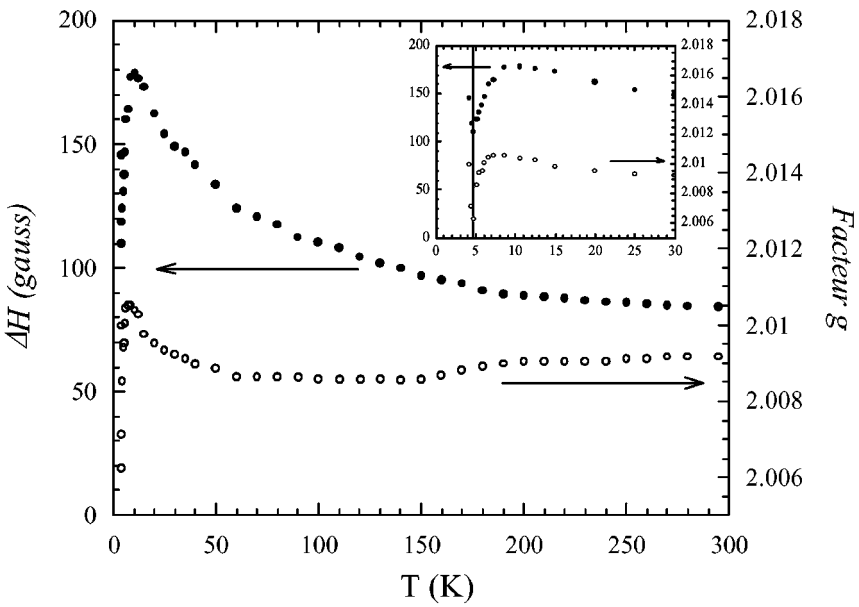


**FIG. 5.** Temperature dependence of the EPR linewidth ($\Delta H$) and the $g$ factor in the $b$ direction for $[Cp_2Mo(dmit)][Br]$. (Insect) Expansion of the low-temperature region.

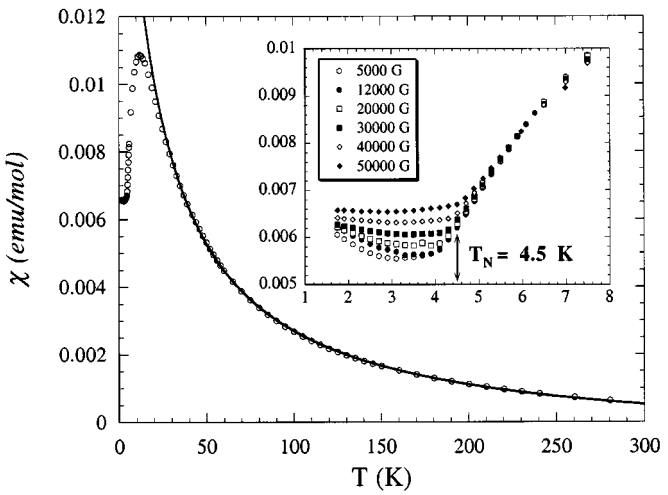


**FIG. 6.** Temperature dependence of the magnetic susceptibility for $[Cp_2Mo(dmit)][Br]$ at 5000 G. The solid line is the best fit obtained using the Curie–Weiss law down to 30 K. (Inset) Expansion of the low-temperature region for different magnetic fields.

exhibits Curie–Weiss behavior down to 30 K as already deduced from the EPR data. The fit of the data gives an estimation of the Curie and Weiss constants. The Curie constant is found to be $C = 0.38$ emu K mol$^{-1}$, which is in agreement with the presence of a $S = \frac{1}{2}$ magnetic spin ($C_{\text{theo}} = 0.375$ emu K mol$^{-1}$) on the radical cation. The calculated Weiss constant is $\theta = -19$ K as already estimated from EPR data and compares favorably with the sum of the exchange interaction roughly estimated from the Hückel calculation (*vide supra*). Below 30 K, the magnetic susceptibility reaches a maximum at 12 K then decreases abruptly as already observed in EPR. As expected for a paramagnetic phase (with $S = \frac{1}{2}$), the magnetic susceptibility is independent of the applied magnetic field down to 5 K. At lower temperature (inset of Fig. 6), around 4.5 K, a field dependence is found, indicative of the occurrence of an antiferromagnetic ground state. The presence of a small amount of ferromagnetic impurities in the sample[1] prevents the determination of the spin-flop field, which seems to be relatively high due to fact that the susceptibility still increases at 50,000 G in the antiferromagnetic region (inset Fig. 6). Below 4.5 K, the magnetic susceptibility measurements confirm the presence of an antiferromagnetic order suggested by the EPR measurements.

[1]The presence of a small amount of ferromagnetic impurity is often found in these compounds. The field dependence of the susceptibility is strongly disturbed by this contribution especially at low field. A ferromagnetic correction was applied in the temperature dependence by translating the curves at different fields on the high-field measurements (5 T) for which this contribution is negligible.

## 4. CONCLUSIONS

These two salts confirm the extremely high flexibility of the $Cp_2Mo(dmit)$ complex in its cation radical salts when faced with various anions of different size and shape. The very low energy cost for folding the $MoS_2C_2$ metallacycle inferred from our recent *ab initio* calculations predicts a folding between 0° and 35° at the expense of less than 1 kcal mol$^{-1}$. This result is experimentally verified here with large $\theta$ values of 23.21(5)° in the $BF_4^-$ salt and 30.45(4)° in the $Br^-$ salt while smaller folding angles between 0° and 10° were previously observed in the $TCNQF_4^{-\cdot}$ and $MF_6^-$ ($M$ = P, As, Sb) salts. While such small anions as $Br^-$, $BF_4^-$, $PF_6^-$, $AsF_6^-$, and $SbF_6^-$ often afford isostructural series with TTF-type donors (TTF for tetrathiafulvalene), the extreme sensitivity of the $Cp_2Mo(dmit)$ complex leads to very different structures and accordingly different magnetic behaviors, isolated dimers, spin ladders, or ordered three-dimensional antiferromagnets.

## ACKNOWLEDGMENTS

We thank C. Lenoir at the Laboratoire de Physique des Solides in Orsay for preliminary electrocrystallisation experiments and J. Amiell at the CRPP, Pessac for his help with the EPR experiments.

## REFERENCES

1. J. A. McCleverty, *Prog. Inorg. Chem.* **10,** 49 (1968).
2. K. Wang and E. I. Stiefel, *Science* **291,** 106 (2001).
3. P. Cassoux, L. Valade, H. Kobayashi, A. Kobayashi, R. A. Clark, and A. E. Underhill, *Coord. Chem. Rev.* **110,** 115 (1991); A. E. Pullen and R.-M. Olk, *Coord. Chem. Rev.* **188,** 211 (1999).
4. L. Brossard, M. Ribault, L. Valade, and P. Cassoux, *Physica B & C* **143,** 378 (1986); H. Tanaka, Y. Okano, H. Kobayashi, W. Suzuki, and A. Kobayashi, *Science* **291** (2001).
5. M. Bousseau, L. Valade, M.-F. Bruniquel, P. Cassoux, M. Garbauskas, L. V. Interrante, and J. Kasper, *New. J. Chem.* **8,** 3 (1984).
6. M. Fourmigué, *Coord. Chem. Rev.* **178–180,** 823 (1998)
7. M. Fourmigué, C. Lenoir, C. Coulon, F. Guyon, and J. Amaudrut, *Inorg. Chem.* **34,** 4979 (1995).
8. M. Fourmigué, B. Domercq, I. V. Jourdain, P. Molinié, F. Guyon, and J. Amaudrut, *Chem. Eur. J.* **9,** 1714 (1998). The folding angle of the $MoS_2C_2$ metallacycle along the S–S hinge is defined as the angle between the mean planes defined by the $MoS_2$ and $S_2C_2$ fragments respectively.
9. (a) R. Clérac, M. Fourmigué, J. Gaultier, Y. Barrans, P.-A. Albouy, and C. Coulon, *Eur. Phys. J. B* **9,** 431 (1999); (b) R. Clérac, M. Fourmigué, J. Gaultier, Y. Barrans, P.-A. Albouy, and C. Coulon, *Eur. Phys. J. B* **9,** 445 (1999).
10. P. Batail, K. Boubekeur, M. Fourmigué, and J.-C. P. Gabriel, *Chem. Mater.* **10,** 3005 (1998) and references therein.
11. E. A. Boudreaux and L. N. Mulay (Eds.), "Theory and Applications of Molecular Paramagnetism." Wiley, New-York, 1976.
12. M. H. Whangbo and R. Hoffmann, *J. Am. Chem. Soc.* **100,** 6093 (1978).
13. J. Ammeter, H.-B. Bürgi, J. Thibeault, and R. Hoffmann, *J. Am. Chem. Soc.* **100,** 3686 (1978).
14. These interaction energies have proven to be very useful in discussing the electronic structures of many organic charge-transfer salts:

J. M. Williams, J. R. Ferraro, R. J. Thorn, K. D. Douglas, U. Geiser, H. H. Wang, A. M. Kini, and M.-H. Whangbo, *in* "Organic Superconductors," Chap. 8. Prentice–Hall, Engelwood Cliffs, 1992.
15. R. L. Carlin, *in* "Magnetochemistry," Springer-Verlag, Berlin, 1986; B. Bleaney and K. D. Bowers, *Proc. R. Soc. London Ser. A* **214,** 451 (1952).
16. B. E. Myers, L. Berger, and S. Friedberg, *J. Appl. Phys.* **40,** 1149 (1969); W. E. Marsh, K. C. Patel, W. E. Hatfield, and D. J. Hodgson, *Inorg. Chem.* **22,** 511 (1982).
17. J. B. Torrance, *in* "Chemistry and Physics of One Dimensional Metals" (H. J. Keller, Ed.), NATO ASI Series, B25, p. 137. Plenum Press, New York, 1977; J. Hubbard, *Phys. Rev. B* **17,** 494 (1978).
18. G. R. Desiraju and T. Steiner, *in* "The Weak Hydrogen Bond," Oxford Univ. Press, Oxford, 1999.
19. P. D. Beer, D. Hesek, J. Hodacova, and S. E. Stockes, *J. Chem. Soc. Chem. Commun.* 270 (1992); P. D. Beer, D. Hesek, J. E. Kingston, D. K. Smith, S. E. Stokes, and M. G. B. Drew, *Organometallics* **14,** 3288 (1995); P. D. Beer, M. G. B. Drew, A. R. Graydon, D. K. Smith, and S. E. Stokes, *J. Chem. Soc. Dalton Trans.* 403 (1995).
20. T. Steiner, *Acta Crystallogr. Sect. B* **54,** 456 (1988).
21. K. Heuzé, M. Fourmigué, P. Batail, E. Canadell, and P. Auban-Senzier, *Chem. Eur. J.* **5,** 2971 (1999); K. Heuzé, C. Mézière, M. Fourmigué, P. Batail, C. Coulon, E. Canadell, P. Auban-Senzier, and D. Jérome, *Chem. Mater.* **12,** 1898 (2000); O. Dautel and M. Fourmigué, *Chem. Eur. J.*, in press.
22. A. J. Moore, M. R. Bryce, A. S. Batsanov, J. N. Heaton, C. W. Lehman, J. A. K. Howard, N. Roberston, A. E. Underhill, and I. F. Perepichka, *J. Mater. Chem.* **8,** 1541 (1998).
23. B. Domercq, C. Coulon, and M. Fourmigué, *Inorg. Chem.* **40,** 371 (2001).
24. L. Landau and E. Lifchitz, *in* "Elasticity Theory," Mir Ed., Moscow, 1967.